

Hydrogeological settings of a volcanic island (San Cristóbal, Galapagos) from joint interpretation of airborne electromagnetics and geomorphological observations

A. Pryet¹, N. d'Ozouville¹, S. Violette¹, B. Deffontaines², and E. Auken³

¹UPMC Univ. Paris 6 & CNRS, UMR Sisyphe, 4 place Jussieu, 75252 Paris cedex 05, France

²UPE, GTMC Laboratory, Marne-La-Vallée, France

³University of Aarhus, Department of Earth Sciences, HydroGeophysics Group, Høegh-Gulbergs gade 2, 8000 Aarhus, Denmark

Correspondence to: A. Pryet
a.pryet@gmail.com

Abstract. Many volcanic islands face freshwater stress and the situation may worsen with climate change and sea level rise. In this context, an optimum management of freshwater resources becomes crucial, but is often impeded by the lack of data. With the aim of investigating the hydrogeological settings of Southern San Cristóbal Island (Galapagos), we conducted an helicopter-borne, transient
5 electromagnetic survey with the *SkyTEM* system. It provided unprecedented insights in the 3D resistivity structure of this extinct basaltic shield. Combined with remote sensing and fieldwork, it allowed the definition of the first hydrogeological conceptual model of the island. Springs are fed by a series of perched aquifers overlying a regional basal aquifer subject to seawater intrusion. Dykes, evidenced by alignments of eruptive cones at the surface, correspond to sharp sub-vertical contrasts
10 in resistivity in the subsurface, and impound groundwater in a summit channel. Combined with geomorphological observations, AEM is shown to be a useful tool for hydrogeological exploratory studies in complex, poorly known environments. It allows optimal development of land-based geophysical surveys and drilling campaigns.

1 Introduction

15 With increasing population and limited resources, freshwater supply has become a critical issue in many volcanic islands (Falkland and Custodio, 1991; Falkland, 1999). Climate change will most probably be associated with rising temperature and increasing sea level (IPCC, 2007), which can reduce groundwater recharge and intensify seawater intrusion (Falkland, 1999; Underwood et al., 1992). In this context, there is a need for a sustainable management of freshwater resources, which
20 can only be achieved once aquifers are clearly delineated and their interactions with the ocean are sufficiently understood, which is not often the case.

Conditions of groundwater occurrence are often well defined in well-studied islands, where human development has been historically accompanied with the drilling of numerous galleries and boreholes such in the Canary and Hawaiian Islands (Custodio, 2004; Gingerich and Oki, 2000). But
25 the hydrogeological settings are poorly constrained in many other islands where human development is more recent, such as the Galapagos Archipelago (d'Ozouville, 2007a). In these islands, there are few or no drill holes and groundwater monitoring is sparse or **inexistent**. nonexistent

Volcanic islands present peculiar hydrogeological characteristics inherited from their specific geological structure. The bulk of volcanic edifices is composed by lava flows and tephra deposits, which are intruded by dykes in **eruptive** ^{vent} zones (Bardintzeff and McBirney, 2006). Dykes can form
30 impervious sub-vertical barriers to groundwater flow, while red “baked” soils and tuff deposits may form impervious layers sub-parallel to the topography (Custodio, 2004; Singhal and Gupta, 2010).

Geophysics has successfully contributed to groundwater characterization of volcanic environments, in particular with electrical, electromagnetic, and audiomagnetotelluric methods (Aizawa et al., 2009; Descloitres et al., 2000; Gómez-Ortiz et al., 2007; Lénat et al., 2000; Lienert, 1991; MacNeil et al., 2007; Revil et al., 2004). Yet, the development of land-based surveys is often long and costly over large, inaccessible areas. Airborne electromagnetics (AEM) can now tackle the issue and cover extensive study areas in a short lapse of time. Several systems have been developed, measuring in the frequency-domain such as *Resolve* and *DigHEM* by Fugro Airborne Surveys (e.g.
40 Mullen et al. (2007) and Siemon (2009)), and in the time-domain, such as *SkyTEM* (Sørensen and Auken, 2004) or *VTEM* by Geotech Airborne Inc. AEM surveys have been successfully conducted during the past decades for risk assessment and hydrogeological prospection in various geological contexts (Bosch et al., 2009; Mogi et al., 2009; Steuer et al., 2009; Supper et al., 2009; Viezzoli et al., 2010b), including volcanic (Auken et al., 2009b; Finn et al., 2001, 2007; d'Ozouville et al., 2008).
45 In most of the above-mentioned studies, geophysical data has been interpreted with a substantial set of drill hole and geological data available prior to the survey.

The project *Galapagos Islands Integrated Water Studies* (GIIWS) was initiated in 2002 with the aim of conducting studies in hydrology and promoting a sustainable management of water resources in the Archipelago. In the frame of the GIIWS project, an extensive *SkyTEM* exploratory survey
50 was conducted in 2006 over the island of San Cristóbal. Here, we first describe a newly acquired

geomorphological dataset collected from remote sensing and field work. The AEM geophysical data is then presented in 3D with a newly available interpolation method (Pryet et al., 2011), and a joint interpretation is performed with the geomorphological dataset. From this analysis, the first hydrogeological conceptual model of the island is proposed. Finally, we discuss the hydrogeological implications and issues related to groundwater characterization based on resistivity mapping in volcanic contexts.

2 Study area

2.1 Geology

San Cristóbal is a basaltic island located on the Nazca oceanic plate, at the eastern end of the Galapagos Archipelago. The island has an elongated shape, 50 km long in the SW-NE direction and 14 km in SE-NW, for a total surface of 558 km². It can be divided into an older southwestern sub-region where volcanic activity coalesced to form a major shield culminating at 710 m above sea level (a.s.l), and a younger flat and arid sub-region to the northeast (Geist et al., 1986). This study focuses on the older, inhabited southwestern part, where permanent springs and streams are present (Figs. 1 and 2).

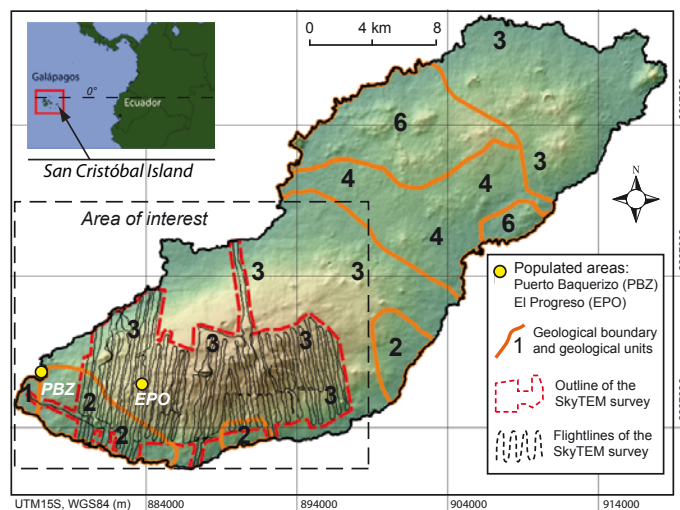


Fig. 1: Geographical settings of San Cristóbal Island. Shaded relief map from the SRTM digital elevation model (Rabus et al., 2003). Geological boundaries from Geist et al. (1986), with ages from the older (1, 2.3 Ma) to younger (6, historical) basaltic formations. Age 2 are reversely polarized flows (>0.78 Ma) and age 3 to 6 are normally polarized (<0.78 Ma).

Reversely polarized flows of the Matuyama epoch (> 0.78 Ma) outcrop at the base of the southwestern shield (Age 2, Fig. 2), but most of the volcano is covered by younger lava flows of the subsequent *Bruhnes* epoch (Age 3, Fig. 2). Eruptions were relatively continuous and characterized

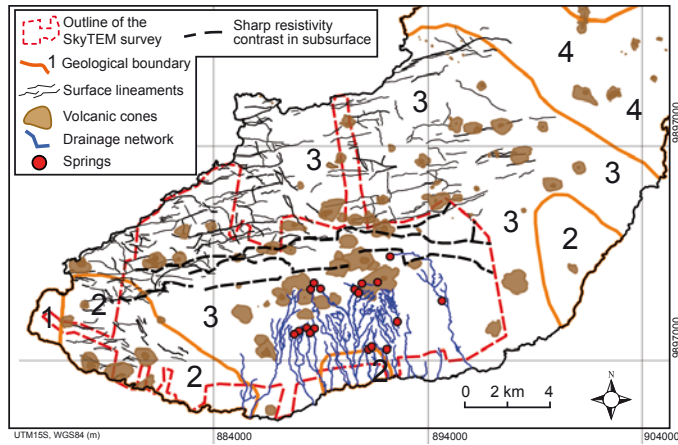


Fig. 2: Surface morphology of the southwestern shield of San Cristóbal island. Geological boundaries from Geist et al. (1986), see caption of Fig. 1 for details. Drainage network, surface lineaments and volcanic cones were mapped from the Google Earth® SPOT imagery and SRTM DEM. Black dashed lines underline major resistivity offsets in the 3D geophysical model (Fig. 5).

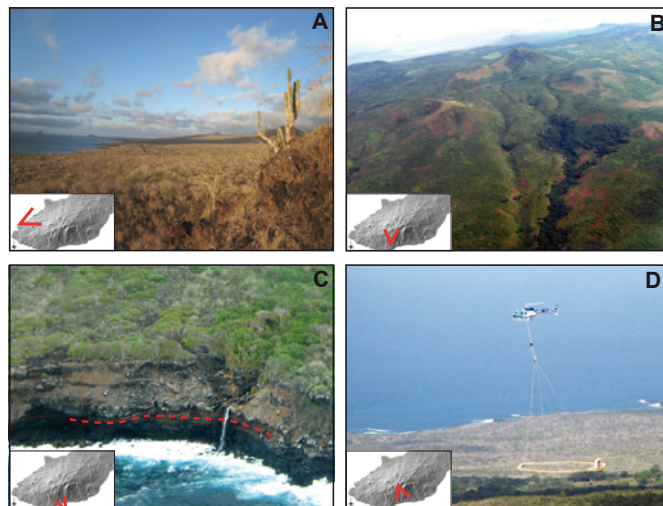


Fig. 3: Photographs of the southern shield of San Cristóbal Island. (A) The dry leeward slopes covered by shrubs and cactus. (B) *San Joaquín* volcanic cone, the topography is incised by streams fed by springs. (C) Perched stream over a red “baked” soil layer (underlined with a red dashed line). (D) The helicopter carrying a frame with the SkyTEM transmitter and receiver coils. Photographs GIIWS project.

with
by moderately thick (1 to 3 m) *pahoehoe* and *aa'* flows (Geist et al., 1986), locally interbedded by
red “baked” soils (d’Ozouville, 2007b). Pyroclastic material forms an exceedingly small part of the
70 volume of the volcano, but at least 10 m of tephra was deposited over the entire summit during the
culminating eruptions some 600,000 years ago (Geist et al., 1986). Few dykes naturally outcrop on
San Cristóbal, but their position may be inferred from their superficial expressions: eruptive fissures
and cones. When cones are elongated or aligned, they are likely to reveal the presence of dyke
swarms (Acocella and Neri, 2009; Chadwick and Howard, 1991).

75 A comprehensive map of volcanic cones and surface lineaments was completed from the geomor-
phological map provided by Ing (1989), Google Earth ® images and the Shuttle Radar Topography
Mission (SRTM DEM) (Rabus et al., 2003) (Fig. 2). Antithetic normal faults intruded by dykes are
evidence of a NNW-SSE extensional extensive tectonic stress, which allowed the co-evolution of faults and
controlled the position of the eruptive zones. Cones do not align along a single rift zone, but are
80 organized along several WSW-ENE alignments and form an elongated ellipsoid at the summit.

2.2 Climate

The climate of the Galapagos Islands is relatively dry with respect to its equatorial location (Colin-
vaux, 1972). Rainfall at low elevation is particularly weak, with a median annual total of 343 mm
(1950-2005, INHAMI) at Puerto Baquerizo (6 m a.s.l.). There is a marked contrast between the
85 southern slopes exposed to the south-east trade-winds where vegetation is scant, and the north-
ern drier slopes covered by spiny shrubs and cactuses (Ing, 1989) (Fig. 3, A and B). With the humid
conditions prevailing in the highlands, the tephra deposits at the summit of San Cristóbal Island
were rapidly weathered to form a thick poorly permeable soil cover (Adelinet et al., 2008; Geist
et al., 1986).

90 Only short-term climatic records are available in the highlands, but the climate of San Cristóbal
is expected to share common patterns with the neighbouring better-studied Santa Cruz Island. On
the windward side, the rainfall orographic gradient was estimated to ca. 415 mm yr⁻¹ per 100 m
elevation from the coast up to the elevation of 440 m a.s.l. (d’Ozouville, 2007b; Pryet et al., 2012).
On the basis of these values, Under these hypotheses, the median annual total along the windward side of San Cristóbal was is
95 estimated to 1580 mm (Pryet, 2011).

2.3 Springs and streams

The mapping of the drainage network provided by Ing (1989) was improved and completed with
air photographs and the high resolution images available on Google Earth ®. The topography of
Southern San Cristobal is incised by numerous ravines, many of which are dry (Fig. 3, B). Intense
100 rainfall events, particularly severe during El Niño years, lead to surface runoff with strong erosional
potential. On the central southern windward slope, the concentration of ravines is the densest and
streamflow is fed by perennial springs. At least six streams reach the sea on a per capita basis (3, C),

which is a unique feature in the Galapagos Archipelago. But due to infiltration losses through river beds, streamflow can decrease downstream and some of the rivers dry before reaching the ocean (Adelinet, 2005; d'Ozouville, 2007b).

Overcoming difficulty of access to the field and temporal variability in the existence of some of the springs, a GPS campaign was carried out resulting in a near-comprehensive map of major springs (Adelinet, 2005) (Fig. 2). Springs are located at slope breaks (depression springs) or at the outcropping of impermeable layers such as red “baked” soil (contact springs) (Fetter, 1994). Springs are poorly mineralized, with electrical conductivities ranging between 30 and 170 $\mu\text{S}\cdot\text{cm}^{-1}$ (Adelinet, 2005). No hydrothermal activity is reported on the island, only traces of extinct fumaroles with white deposit (sodium sulfate) can be identified (Simkin, 1984).

3 Airborne electromagnetic survey

3.1 Data acquisition and processing

The airborne electromagnetic survey was conducted in May 2006 with the SkyTEM system (Sørensen and Auken, 2004) (Fig. 3, D). The average flight speed was 45 $\text{km}\cdot\text{hr}^{-1}$ and the flight altitude of the rig was 35-45 m above the ground surface. About 23,000 soundings were performed in 8 days along 900 km of flight lines, with a sounding every 25-50 m. Flight lines were generally oriented N-S with a spacing of 200 m (Fig. 1). The survey focused on the southern windward slopes, but a few lines were flown cross-island to obtain a full picture of the fresh-saltwater interface.

The system transmits two magnetic moments, a low moment for the resolution of the near surface layers and a high moment for the resolution of the deeper layers. The data filtering is designed to enhance near-surface resistivity variations by avoiding any smoothing of the early-time data while late-time data are more severely filtered to obtain as much penetration depth as possible (Auken et al., 2009a).

Soundings were inverted to 4-layer 1D vertical resistivity models with the spatially constrained inversion scheme (SCI) (Viezzoli et al., 2008, 2010a). With this method, local resistivity models are constrained by neighbouring soundings. This enhances the resolution of model parameters (i.e. layer resistivities and interfaces), which are not well resolved in an independent inversion. The inversion models were then interpolated to form a coherent 3D grid of resistivity with the methodology detailed by Pryet et al. (2011). To obtain a finite 3D model, the thickness of the last layer was arbitrarily fixed to 2.5 times the thickness of the overlying 3rd layer. The 3D grid of resistivity was then imported into Paraview®, which allowed flexible visualization and volume extraction based on resistivity thresholds.

135 3.2 Results

Resistivities of the 4-layer 3D model range between ca. 1 and 3000 ohm.m. The depth of penetration was approximated from the depth to the last geophysical interface, i.e. between the 3rd and 4th resistivity layers, and ranged between 20 and 550 m with a mean of 165 m below ground level.

3.2.1 Contrasts between the windward and leeward sides

140 The geophysical survey reveals a striking contrast in resistivity between windward and leeward sides of San Cristóbal Island (Fig. 4 and 5). Above sea level, formations of the northern side are resistive (800-3000 ohm.m), which is compatible with unweathered, unsaturated basaltic formations (Descloitres et al., 1997, 2000). In contrast, the bulk of the southern, windward side presents low to intermediate resistivity (10-200 ohm.m), compatible with formations subjected to various degree of
145 weathering or saturation (Descloitres et al., 1997; Lénat et al., 2000; Müller et al., 2002).

No constructional process can be invoked to explain such a contrast between the windward and leeward sides. Erupted lavas and pyroclastics deposits of the two sides shared identical chemical and physical properties at the date of their emplacement (Geist et al., 1986). The only difference that can be expected between the two sides is a higher amount of volcanic ash blown by the trade-winds to the north, but these materials are easily weathered and would reduce resistivity in the north, contrary
150 to what is observed.

The contrast in resistivity can therefore be explained by differential weathering induced by the contrasting climatic conditions at the surface and the presence of groundwater in the subsurface. Weathering confers a low resistivity to basaltic formations due to the presence of clayey secondary
155 minerals (Eggleton et al., 1987; Gislason et al., 1993). As weathering rates are enhanced by water percolation, areas with higher recharge rates are prone to enhanced rock weathering (Adelinet et al., 2008; Gislason et al., 1993; Hay and Jones, 1972; Van der Weijden and Pacheco, 2003). Similarly to the neighbouring Santa Cruz Island (d'Ozouville et al., 2008), contrasting climatic conditions in San Cristóbal induced marked differences in rock weathering between the windward and leeward sides.

160 3.2.2 Imprints of salt water intrusion

Cross-sections (Fig. 4) reveal a very conductive unit (1-15 ohm.m) standing close to, or below sea level around the central shield. This is the typical signature of seawater intrusion beneath a *basal aquifer* (Auken et al., 2009b), which is confirmed by field observation. The aquifer outcrops at the bottom of a pit mine near Puerto Baquerizo (Fig. 1) and the water is brackish ($\chi = 28 \text{ mS.cm}^{-1}$).

165 A map of the Salt Water Interface (SWI) was derived from the elevation of the upper interface of the lower, very conductive ($< 15 \text{ ohm.m}$) geophysical layer (Fig. 6). This SWI map provides only an estimate of indicative values, as the actual interface between sea- and freshwater is often diffuse, and vertical salinity profiles measured in monitoring wells are necessary to better define the actual thickness of

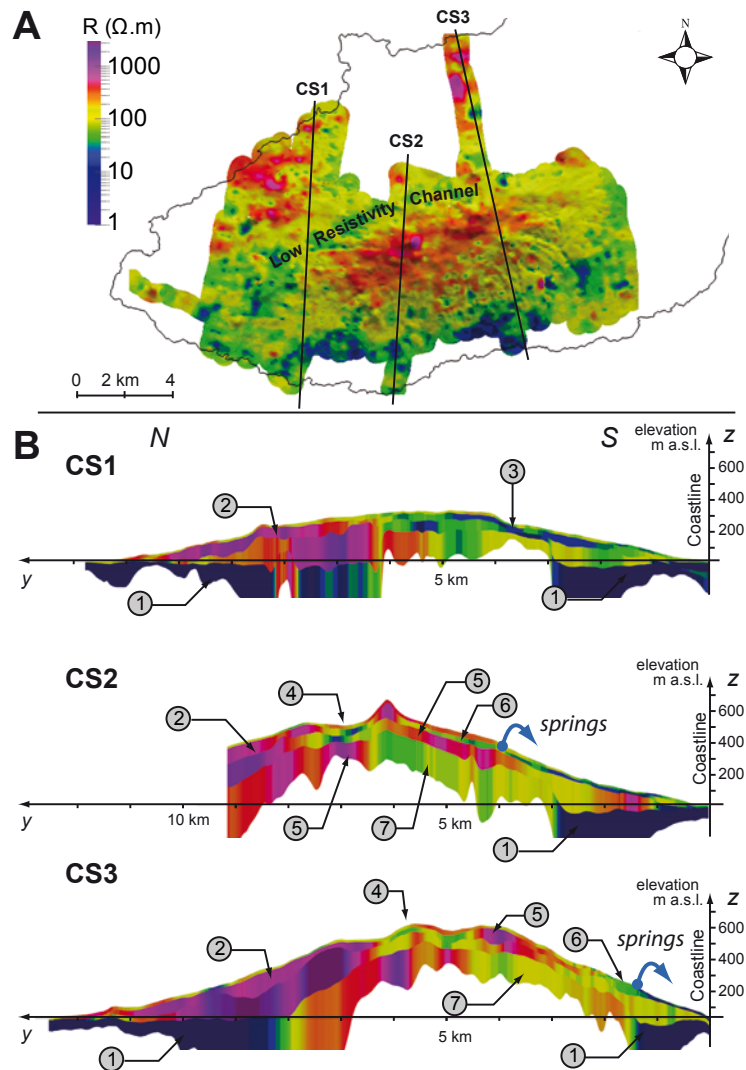


Fig. 4: (A) Surface resistivity of the 4-layer SkyTEM resistivity model. (B) Corresponding cross-sections. 1. Seawater intrusion ($< 15 \text{ ohm.m}$), 2. Undifferentiated, unweathered, unsaturated volcanic formations ($> 400 \text{ ohm.m}$), 3. Very low resistivity formation ($10\text{-}70 \text{ ohm.m}$) expanding from the summit area, 4. Buried low resistivity channel ($30\text{-}100 \text{ ohm.m}$), 5. Massive lava flows ($> 400 \text{ ohm.m}$), 6. Perched aquifer ($30\text{-}100 \text{ ohm.m}$) 7. Undifferentiated, unsaturated weathered volcanic formations ($100\text{-}400 \text{ ohm.m}$). The shading with depth reflects the approximative depth of investigation.

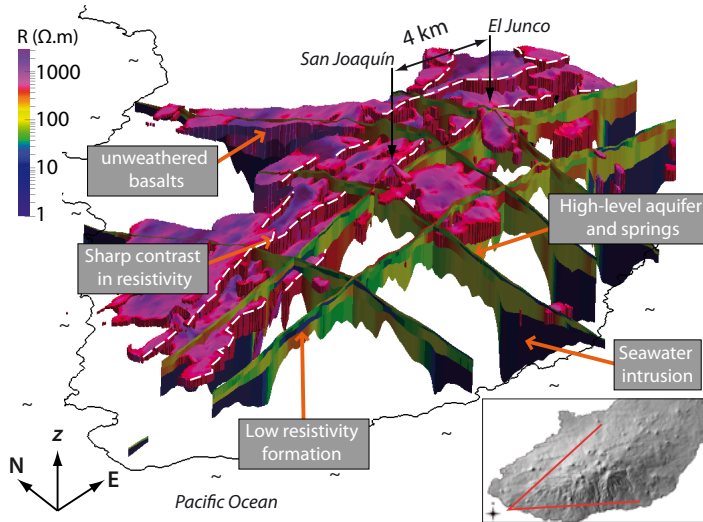


Fig. 5: 3D view of the SkyTEM 4-layer resistivity model. The high resistivity extraction (threshold of resistivity $> 400 \text{ ohm.m}$) appears dissected by major offsets, with downthrows up to 100 m (white, dashed lines). The scarps are supposed to be associated with major dikes and form the lateral boundaries of the buried low-resistivity channel (Section 3.2.4)

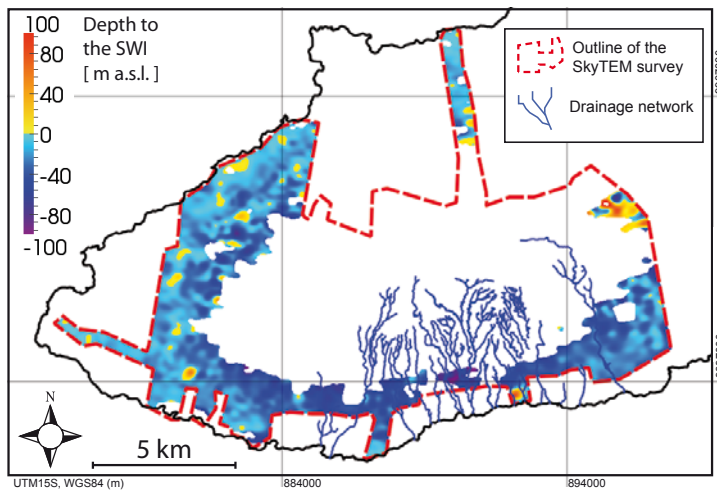


Fig. 6: Depth to the *Salt Water Interface* (SWI) inferred from the 4 layer resistivity model. SWI elevation is estimated from the elevation of the upper interface of the deep, very conductive geophysical layers ($< 15 \text{ ohm.m}$). Values above sea level are artefacts and should be disregarded.

the freshwater lens (Izuka and Gingerich, 1998). The SWI appears shallower on the dry northern and western slopes (0-30 m below sea level) and deeper at the southern windward side (0-100 m below sea level). The SWI is particularly deep at the center of the southern watershed, 1.6 km from the coast, where surface drainage network concentrates (Fig. 6). In the central part of the surveyed area, the SWI is too deep with respect to ground level to be detected by SkyTEM soundings.

The freshwater lens could not be resolved with the 4-layer inversion model, but an estimate of the watertable elevation can be inferred from the SWI map (Lienert, 1991). Assuming hydrostatic equilibrium and no mixing between fresh- and salt water, the Ghyben-Herzberg equation relates the elevation of the watertable to the SWI depth by a ratio of 1 to 40 (see e.g. Bear (1999)). This method is not accurate, but provides an order of magnitude of the watertable elevation (Izuka and Gingerich, 1998). At the windward side of the island, the depth to the SWI is estimated to range between 0 and 100 m below sea level (Fig. 6). This yields a watertable ranging only between 0 and 2.5 m above sea level.

3.2.3 High-level groundwater

Numerous springs identified at the surface are located below outcrops of weakly resistive geophysical layers (30-100 ohm.m, greenish colors, Fig. 4). As spring water is poorly mineralized ($\chi = 30$ to $170 \mu\text{S}\cdot\text{cm}^{-1}$), the saturation of the porosity cannot explain alone the observed low rock electrical resistivities. They are attributed to the occurrence of clayey minerals, produced by the alteration of basaltic formations (Eggleton et al., 1987; Gislason et al., 1993).

As shown in Section 3.2.2, the basal aquifer watertable remains at limited elevations (0 - 2.5 m a.s.l.) up to 1.7 km from the coast. The basal aquifer is therefore unlikely to be at the origin of the springs located at ca. 150 m a.s.l., 2 km from the coastline. High-level springs must originate from perched aquifers, disconnected from the basal aquifer, as proposed e.g. for Hawaii (Ingebritsen and Scholl, 1993), Réunion (Join et al., 1997; Violette et al., 1997), and Cape Verde (Heilweil et al., 2009) islands. Perched aquifers can form over impervious units, e.g. ash deposits, and red “baked” soils, which are too thin to be resolved with TEM soundings, but have been identified on coastal cliffs and ravines of San Cristóbal (Fig. 3, C).

3.2.4 Low resistivity channel

In the summit zone, resistive units in the subsurface are markedly resist and reveal a low-resistivity (30-100 ohm.m), WSW-ENE trending buried channel (Figs. 4 and 5). The low resistivity channel is located between 10-100 m below ground level, and locally outcrops without noticeable difference at the surface. Sharp contrast resistivity are highlighted by important vertical scarps (up to 100 m) in the high-resistivity extrusion (Fig. 5). The northern scarp follows the pattern of aligned volcanic cones at the surface, which probably underlines SW-ENE trending dyke swarm (Fig. 2, black dashed lines). Such an alignment is less conspicuous for the southern offset.

The presence of low resistivity formations in the central areas of volcanic islands is often associated with hydrothermally altered hydrothermalized formations (Aizawa et al., 2009; Müller et al., 2002; Revil et al., 2004), but there is no evidence of past or present hydrothermal activity on San Cristóbal. A resistivity of 30-100 ohm.m is compatible with saturated, weathered basaltic formations (see Section 3.2.3), and the central, buried low-resistivity channel can be interpreted as a dyke-impounded aquifer, which is commonly observed in other volcanic islands (Custodio, 2004; Stearns and McDonald, 1947; Takasaki and Mink, 1981). As detailed by Bret et al. (2003) from observation performed in an horizontal tunnel in La Reunion Island, the occurrence of a dyke-impounded aquifer can induce sharp contrast in rock weathering. Such a phenomenon can be invoked to explain the sharp transition in resistivity observed in the central zone of San Cristóbal.

The central low-resistivity channel dips westward and terminates expanding over the southwestern flank of the main shield with decreasing resistivities (10-40 ohm.m) (Fig. 4, A and B, CS1-Num. 3). This formation is subparallel to the topography and seems to circumvent volcanic cones. Such a low resistivity domain may be interpreted as the effect of enhanced weathering induced by groundwater flow from the dyke-impounded aquifer. Yet, the resistivities are particularly low and may reveal distinct geological unit such as older lava flows, or colluvial deposits with high clay content.

4 Discussion

4.1 Hydrogeological conceptual model

We
~~The results of the interpretation can be gathered to~~ define the first hydrogeological conceptual model of San Cristóbal (Fig. 7). The freshwater lens is thicker at the windward side, but the water table is expected to remain at low elevation (ca. 0-2.5 m a.s.l.). As a consequence, the basal aquifer cannot be invoked to explain the occurrence of springs at high elevation (Section 3.2.2). Springs are more likely associated with perched aquifers developing over impervious layers, such as red “baked” soils (Section 3.2.3). The buried low-resistivity channel revealed in the summit zone can be interpreted as a dyke-impounded aquifer (Section 3.2.4). This hydrogeological configuration, often referred as the *Hawaiian model* in the literature (Custodio, 2004; Stearns and McDonald, 1947), has been identified in similar volcanic islands such as the Hawaiian, Azores, and Réunion islands (Cruz and França, 2006; Ingebritsen and Scholl, 1993; Violette et al., 1997; Join et al., 1997).

4.2 Resistivity mapping in basaltic environments

~~On the basis of a study of small~~
~~After a study on rock samples,~~ Perrier and Froidefond (2003) showed that the electrical properties of volcanic formations are mainly controlled by secondary minerals. The contrast in resistivity between the windward and leeward sides of San Cristóbal Island also illustrates this result: marked differences in resistivity between the two sides are interpreted as the consequence of differential weathering (Section 3.2.1).

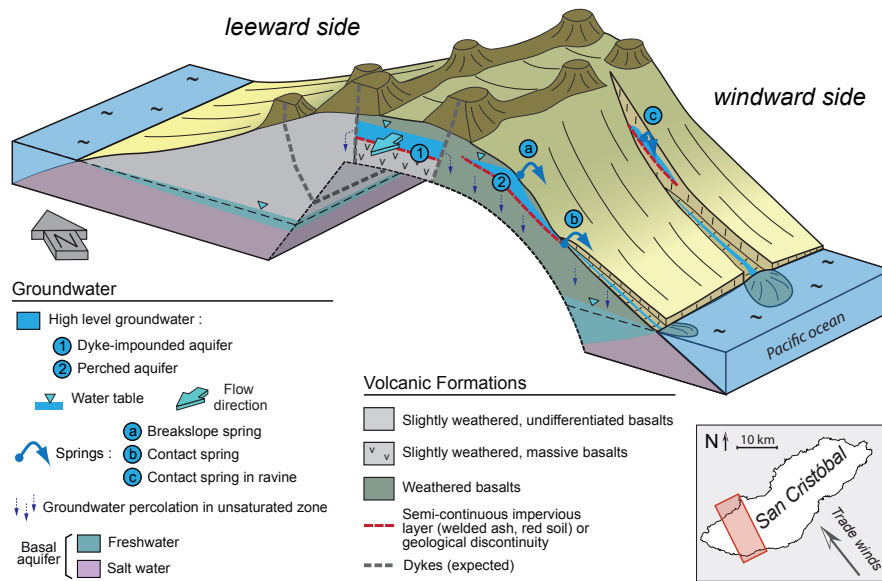


Fig. 7: Hydrogeological conceptual model of San Cristóbal Island, inferred from geomorphological observations and airborne electromagnetic survey. The configuration is asymmetric, the basal aquifer is thin and basalt are weakly weathered in the northern leeward side, while the basal aquifer is thicker and basalts are weathered in the southern, windward side. Springs are fed by perched aquifers and a dyke-impounded aquifer may be present in the central area.

These results highlight that resistivity mapping in volcanic environments may result in the mapping of weathering. In this context, saturation with freshwater may not be unambiguously identified.

240 The occurrence of groundwater can yet be detected indirectly, since the water table often corresponds to a contrast in rock weathering (Keller et al., 1979; Lienert, 1991). On San Cristóbal Island for instance, the presence of clayey minerals in the saturated levels explains that perched aquifers at the origin of springs in San Cristóbal are associated with particularly low resistivities (30-100 ohm.m), though groundwater is poorly mineralized (30 and 170 $\mu\text{S}\cdot\text{cm}^{-1}$).

245 This study shows that exploratory AEM surveys are efficient for resistivity imaging over large inaccessible areas. In volcanic islands, the implementation of AEM survey allows an efficient mapping of intruding salt water and weathered formations, that are both characterized by low resistivities. The geometry of aquifers may be inferred from resistivity maps, but their resistivity signature depends on the degree of weathering of the host rocks. As a consequence, the definition of an hydrogeological
 250 conceptual model requires additional field observations.

5 Conclusions

The *SkyTEM* survey conducted over San Cristóbal Island provided a map of resistivity over 140 km² with a mean penetration depth of 165 m below ground level. The survey revealed a marked contrast in subsurface resistivity between the windward and leeward sides, which was explained by differential weathering induced by contrasting climatic conditions at the surface. Combined with geomorphological observations, geophysical data provided valuable insights into the hydrogeological settings. The first hydrogeological conceptual model was proposed for San Cristóbal Island, it can be related to the *Hawaiian model* for volcanic islands: a basal aquifer subject to seawater intrusion, series of perched aquifer, and a dyke impounded aquifer in the summit zone. The hydrogeological conceptual model can now be validated with land-based geophysical surveys directly sensitive to groundwater occurrence (proton magnetic resonance, self-potential) and a drilling campaign focused in the areas of interest.

Acknowledgements. This study was performed within the framework of the project *Galapagos Islands Integrated Water Studies* (GIIWS), funded by the Agence Nationale de la Recherche (ANR-blanc 2010 GIIWS Ref. 601-01). The Charles Darwin Research Station and the Galapagos National Park collaborated to the 2006 *SkyTEM* survey in Galápagos, which was funded by Fondation de France, Fondation Véolia Environnement, Fondation Schlumberger-SEED, Chancellerie des Universités de Paris, UGAFIP-BID and Municipality of Santa Cruz. The authors would like to thank David Fauchet, Wafa Ramdani and Fabian Lindner for their participation in the digitalization of cones, fractures and rivers, which was performed under Qgis (<http://www.qgis.org>).

270 References

- Inventario cartografico de los recursos naturales, geomorfologia, vegetacion, ecologicos, y biofisicos de las islas Galápagos, Ecuador, Tech. rep., Ingala and Pronareg and Orstom, 1989.
- Acocella, V. and Neri, M.: Dike propagation in volcanic edifices: Overview and possible developments, *Tectonophysics*, 471, 67–77, 2009.
- 275 Adelinet, M.: Etude hydrologique des bassins versants de l'île de San Cristóbal (Galapagos, Equateur), Master's thesis, ENS Paris and UPMC Univ. Paris 6, Sisyphe Lab., 2005.
- Adelinet, M., Fortin, J., d'Ozouville, N., and Violette, S.: The relationship between hydrodynamic properties and weathering of soils derived from volcanic rocks, Galapagos Islands (Ecuador), *Environ. Geol.*, 56, 45–58, 2008.
- 280 Aizawa, K., Ogawa, Y., and Ishido, T.: Groundwater flow and hydrothermal systems within volcanic edifices: Delineation by electric self-potential and magnetotellurics, *J. Geophys. Res. - Sol. Ea.*, 114, B01 208, 2009.
- Auken, E., Christiansen, A., Westergaard, J., Kirkegaard, C., Foged, N., and Viezzoli, A.: An integrated processing scheme for high-resolution airborne electromagnetic surveys, the SkyTEM system, *Explor. Geophys.*, 40, 184–192, 2009a.
- 285 Auken, E., Violette, S., d'Ozouville, N., Deffontaines, B., I. Sørensen, K., Viezzoli, A., and de Marsily, G.: An integrated study of the hydrogeology of volcanic islands using helicopter borne transient electromagnetic: Application in the Galapagos Archipelago, *C. R. Geosci.*, 341, 899–907, 2009b.
- Bardintzeff, J. and McBirney, A.: *Volcanology*, Jones and Barlett, 2006.
- Bear, J.: Seawater intrusion in coastal aquifers: Concepts, methods, and practices, chap. Conceptual and Mathematical Modeling, pp. 163–191, Springer, 1999.
- 290 Bosch, J., Bakker, M. J., Gunnink, J., and Paap, B.: Airborne electromagnetic measurements as basis for a 3D geological model of an Elsterian incision, *Z. Dtsch. Ges. Geowiss.*, 160, 249–258, 2009.
- Bret, L., Join, J., Legal, X., Coudray, J., and Fritz, B.: Clays and zeolites in the weathering of a basaltic tropical shield volcano (Le Piton des Neiges, Reunion Island), *C. R. Geosci.*, 335, 1031–1038, 2003.
- 295 Chadwick, W. and Howard, K.: The pattern of circumferential and radial eruptive fissures on the volcanoes of Fernandina and Isabela islands, Galapagos, *B. Volcanol.*, 53, 259–275, 1991.
- Colinvaux, P.: Climate and the Galapagos islands, *Nature*, 240, 17–20, 1972.
- Cruz, J. and França, Z.: Hydrogeochemistry of thermal and mineral water springs of the Azores archipelago (Portugal), *J. Volcanol. Geoth. Res.*, 151, 382–398, 2006.
- 300 Custodio, E.: Hydrogeology of volcanic rocks, chap. Hydrogeology of volcanic rocks, pp. 395–425, UNESCO, Paris, 2004.
- Descloitres, M., Ritz, M., Robineau, B., and Courteaud, M.: Electrical structure beneath the eastern collapsed flank of Piton de la Fournaise volcano, Reunion Island: Implications for the quest for groundwater, *Water Resour. Res.*, 33, 13–19, 1997.
- 305 Descloitres, M., Guérin, R., Albouy, Y., Tabbagh, A., and Ritz, M.: Improvement in TDEM sounding interpretation in presence of induced polarization. A case study in resistive rocks of the Fogo volcano, Cape Verde Islands, *J. of Appl. Geophys.*, 45, 1–18, 2000.
- d'Ozouville, N.: Agua dulce: la realidad de un recurso crítico, Informe Galápagos 2006-2007, pp. 150–160, 2007a.
- 310 d'Ozouville, N.: Etude du Fonctionnement Hydrologique Dans les Iles Galápagos : caractérisation d'un milieu volcanique insulaire et préalable à la gestion de la ressource., Ph.D. thesis, Université Paris 6 Pierre et Marie Curie, 2007b.
- d'Ozouville, N., Auken, E., Sorensen, K., Violette, S., de Marsily, G., Deffontaines, B., and Merlen, G.: Extensive perched aquifer and structural implications revealed by 3D resistivity mapping in a Galapagos volcano, *Earth and Planet. Sc. Lett.*, 269, 517–521, 2008.
- 315 Eggleton, R., Foudoulis, C., and Varkevisser, D.: Weathering of basalt: changes in rock chemistry and mineralogy, *Clay. Clay Miner.*, 35, 161–169, 1987.
- Falkland, A.: Tropical Island Hydrology and Water Resources Current Knowledge and Future Needs, in: Hydrology and water management in the humid tropics. Proceedings of the Second International Colloquium, Panama, 1999.
- 320 Falkland, A. and Custodio, E.: Guide on the Hydrology of Small Islands. Studies and Reports in Hydrology., Unesco, Paris, 1991.
- Fetter, C.: *Applied Hydrogeology*, Prentice Hall, 1994.
- Finn, C., Sisson, T., and Deszcz-Pan, M.: Aerogeophysical measurements of collapse-prone hydrothermally altered zones at Mount Rainier volcano, *Nature*, 409, 600–603, 2001.
- 325

- Finn, C., Deszcz-Pan, M., Anderson, E., and John, D.: Three-dimensional geophysical mapping of rock alteration and water content at Mount Adams, Washington: Implications for lahar hazards, *J. Geophys. Res. - Sol. Ea.*, 112, B10204, 2007.
- 330 Geist, D., McBirney, A., and Duncan, R.: Geology and petrogenesis of lavas from San Cristobal Island, Galapagos Archipelago, *Bull. Geol. Soc. Am.*, 97, 555–566, 1986.
- Gingerich, S. B. and Oki, D. S.: Ground Water in Hawaii, Tech. rep., USGS Pacific Islands Water Science Center, 2000.
- Gislason, S., Veblen, D., and Livi, K.: Experimental meteoric water-basalt interactions: Characterization and interpretation of alteration products, *Geochim. Cosmochim. Ac.*, 57, 1459–1471, 1993.
- 335 Gómez-Ortiz, D., Martín-Velázquez, S., Martín-Crespo, T., Márquez, A., Lillo, J., López, I., Carreño, F., Martín-González, F., Herrera, R., and De Pablo, M.: Joint application of ground penetrating radar and electrical resistivity imaging to investigate volcanic materials and structures in Tenerife (Canary Islands, Spain), *J. of Appl. Geophys.*, 62, 287–300, 2007.
- 340 Hay, R. and Jones, B.: Weathering of basaltic tephra on the island of Hawaii, *Geol. Soc. Am. Bull.*, 83, 317–332, 1972.
- Heilweil, V. M., Solomon, D. K., Gingerich, S. B., and Verstraeten, I. M.: Oxygen, hydrogen, and helium isotopes for investigating groundwater systems of the Cape Verde Islands, West Africa, *Hydrogeol. J.*, 17, 1157–1174, 2009.
- Ingebritsen, S. and Scholl, M.: The hydrogeology of Kilauea volcano, *Geothermics*, 22, 255–270, 1993.
- 345 IPCC: Contribution of Working Groups I, II and III to the Fourth Assessment Report of the Intergovernmental Panel on Climate Change, vol. 104, IPCC, Geneva, Switzerland, 2007.
- Izuka, S. and Gingerich, S.: Estimation of the depth to the fresh-water/salt-water interface from vertical head gradients in wells in coastal and island aquifers, *Hydrogeol. J.*, 6, 365–373, 1998.
- 350 Join, J., Coudray, J., and Longworth, K.: Using principal components analysis and Na/Cl ratios to trace groundwater circulation in a volcanic island: the example of Reunion, *J. Hydrol.*, 190, 1–18, 1997.
- Keller, G., Grose, L., Murray, J., and Skokan, C.: Results of an experimental drill hole at the summit of Kilauea volcano, Hawaii, *J. Volcanol. Geoth. Res.*, 5, 345–385, 1979.
- Lienert, B.: An Electromagnetic study of Maui's last active volcano, *Geophysics*, 56, 972–982, 1991.
- 355 Lénat, J., Fitterman, D., Jackson, D., and Labazuy, P.: Geoelectrical structure of the central zone of Piton de la Fournaise volcano (Réunion), *B. Volcanol.*, 62, 75–89, 2000.
- MacNeil, R., Sanford, W., Connor, C., Sandberg, S., and Diez, M.: Investigation of the groundwater system at Masaya Caldera, Nicaragua, using transient electromagnetics and numerical simulation, *J. Volcanol. Geoth. Res.*, 166, 217–232, 2007.
- 360 Mogi, T., Kusunoki, K., Kaieda, H., Ito, H., Jomori, A., Jomori, N., and Yuuki, Y.: Grounded electrical-source airborne transient electromagnetic (GREATEM) survey of Mount Bandai, north-eastern Japan, *Explor. Geophys.*, 40, 1–7 Sp.Iss. SI., 2009.
- Mullen, I., Wilkinson, K., Cresswell, R., and Kellett, J.: Three-dimensional mapping of salt stores in the Murray-Darling Basin, Australia: 2. Calculating landscape salt loads from airborne electromagnetic and laboratory data, *Int. J. Appl. Earth Obs.*, 9, 103–115, 2007.
- 365 Müller, M., Hördt, A., and Neubauer, F.: Internal structure of Mount Merapi, Indonesia, derived from long-offset transient electromagnetic data, *J. Geophys. Res. - Sol. Ea.*, 107, B9, 2002.
- Perrier, F. and Froidefond, T.: Electrical conductivity and streaming potential coefficient in a moderately alkaline lava series, *Earth and Planet. Sc. Lett.*, 210, 351–363, 2003.
- 370 Pryet, A.: Hydrogeology of volcanic islands: a case-study in the Galapagos Archipelago, Ph.D. thesis, Université Pierre et Marie Curie, 2011.
- Pryet, A., Ramm, J., Chilès, J.-P., Auken, E., Deffontaines, B., and Violette, S.: 3D resistivity gridding of large AEM datasets: A step toward enhanced geological interpretation, *J. of Appl. Geophys.*, 75, 277 – 283, 2011.
- 375 Pryet, A., Dominguez, C., Fuente Tomai, P., Chaumont, C., d'Ozouville, N., Villacís, M., and Violette, S.: Quantification of cloud water interception along the windward slope of Santa Cruz Island, Galapagos, *Agr. Forest Meteorol.*, 161, 94–106, 2012.
- Rabus, B., Eineder, M., Roth, A., and Bamler, R.: The shuttle radar topography mission—a new class of digital elevation models acquired by spaceborne radar, *Int. Soc. Photogramme.*, 57, 241–262, 2003.
- Revil, A., Finizola, A., Sortino, F., and Ripepe, M.: Geophysical investigations at Stromboli volcano, Italy: implications for ground water flow and paroxysmal activity, *Geophys. J. Int.*, 157, 426–440, 2004.
- 380 Siemon, B.: Levelling of helicopter-borne frequency-domain electromagnetic data, *J. of Appl. Geophys.*, 67, 206–218, 2009.

- Simkin, T.: Geology of Galapagos, *Biol. J. Linn. Soc.*, 21, 61–75, 1984.
- Singhal, B. and Gupta, R.: Applied Hydrogeology of Fractured Rocks, chap. Hydrogeology of Volcanic Rocks, pp. 257–268, Springer Netherlands, 2010.
- 385 Sørensen, K. and Auken, E.: SkyTEM - A new high-resolution helicopter transient electromagnetic system, *Explor. Geophys.*, 35, 191–199, 2004.
- Stearns, H. and McDonald, G.: Geology and groundwater resources of the island of Hawaii, Hawaii Division of Hydrography Bulletin, 9, 1947.
- 390 Steuer, A., Siemon, B., and Auken, E.: A comparison of helicopter-borne electromagnetics in frequency- and time-domain at the Cuxhaven valley in Northern Germany, *J. of Appl. Geophys.*, 67, 194–205, 2009.
- Supper, R., Motschka, K., Ahl, A., Bauer-Gottwein, P., Gondwe, B., Alonso, G., Romer, A., Ottowitz, D., and Kinzelbach, W.: Spatial mapping of submerged cave systems by means of airborne electromagnetics: an emerging technology to support protection of endangered karst aquifers, *Near Surf. Geophys.*, 7, 613–627, 2009.
- 395 Takasaki, K. and Mink, J.: Evaluation of Major Dike-impounded Ground-water Reservoirs, Island of Oahu, US Department of the Interior, Geological Survey, 1981.
- Underwood, M. R., Peterson, F. L., and Voss, C. I.: Groundwater Lens Dynamic of Atoll Islands, *Water Resour. Res.*, 28, 2889–2902, 1992.
- 400 Van der Weijden, C. and Pacheco, F.: Hydrochemistry, weathering and weathering rates on Madeira islands, *J. Hydrol.*, 283, 122–145, 2003.
- Viezzoli, A., Christiansen, A. V., Auken, E., and Sorensen, K.: Quasi-3D modeling of airborne TEM data by spatially constrained inversion, *Geophysics*, 73, F105–F113, <http://link.aip.org/link/?GPY/73/F105/1>, 2008.
- Viezzoli, A., Munday, T., Auken, E., and Christiansen, A.: Accurate quasi 3D versus practical full 3D inversion of AEM data, *Preview*, 149, 23–31, 2010a.
- 405 Viezzoli, A., Tosi, L., Teatini, P., and Silvestri, S.: Surface water–groundwater exchange in transitional coastal environments by airborne electromagnetics: The Venice Lagoon example, *Geophys. Res. Lett.*, 37, L01402, 2010b.
- Violette, S., Ledoux, E., Goblet, P., and Carbonnel, J.: Hydrologic and thermal modeling of an active volcano: the Piton de la Fournaise, Reunion, *J. Hydrol.*, 191, 37–63, 1997.